

# A Network-Based Model for Decision Making in a Criminal Society

Kym Louie\*, Ian Drayer†, Jiahui Yu†

Mentors: Martin Short† and David Uminsky†

August 4, 2011

## 1 Introduction

Game theory can be applied to the study of criminal behavior as well as economic theory [7] [8]. By modeling how people make decisions in response to criminal activities, we can learn about the progression of criminal behavior within a population, and its dependence on the initial distribution of types of people.

Our model is based on an adversarial evolutionary game introduced by M.B. Short, et. al. [6]. Under this model, we consider an ideal society with four types of citizens. The  $I$  Informants commit crimes but also willing to report crimes and serve as witnesses. The  $V$  Villains commit crimes and never cooperate with the police to serve as witnesses. The  $A$  Apathetics neither commit crimes nor serve as witnesses for crimes. And  $P$  Paladins, do not commit any crimes and are willing to report and serve as witnesses for crimes. Therefore, the total population  $N = I + V + A + P$ .

The systems described in this paper proceed in the same fashion as the system defined by Short, where each turn an attacker is chosen at random however their victim is chosen with given, not necessarily uniform probabilities. Other modifications examined include a wealth accumulation model where individuals will keep the wealth gained through an attack. As with Short's model, the loser of an individual encounter is given the chance to revise their strategy.

The evolution of cooperative behavior is studied by iterating the model until one of two equilibrium states is reached, the "utopian society" in which ( $V + I = 0, P + A = N$ ) there are no criminals, or the "dystopian society" in which ( $P + I = 0$  and  $V + A = N$ ) no criminal activities are reported. Although neither equilibrium state includes Informants, they are the key to the long-term behavior of the population [6]. If no Informants are initially present, then there is a minimal number of Paladins that must be present initially for the

---

\*Harvey Mudd College

†UCLA

population to have a reasonably high chance of reaching the utopian equilibrium. However, even if the number of Paladins is below this threshold, including a small percentage of Informants greatly increases the probability that the utopian equilibrium is reached.

We extend this model by implementing different types of networks within the society. Each individual is represented by a vertex and the vertices are connected to each by edges on a graph. We require that an attacker can only attack someone that they are adjacent to, and that the attack rate is proportional to the weight of each edge.

We will demonstrate the differing wealth distributions for utopian societies and dystopian societies as well as the differing wealth distributions between the network-free model and geographic threshold graphs in both utopia and dystopia. We will also discuss the results of applying Short's model on a variety of networks including networks built on a cycle.

## 2 Three Basic Networks

Three basic networks will be introduced: Erdős-Rényi graphs, Geographic Threshold Graphs, and a 4-regular lattice on a torus <sup>1</sup>. In these networks, attacks committed by players are restricted to players with which they share an edge, effectively limiting a spread of information to certain paths. Due to this, on all of these networks the average time to reach a stable equilibrium is elevated.

Following the introduction of these networks, the behavior of simulated criminal societies on these networks will be compared.

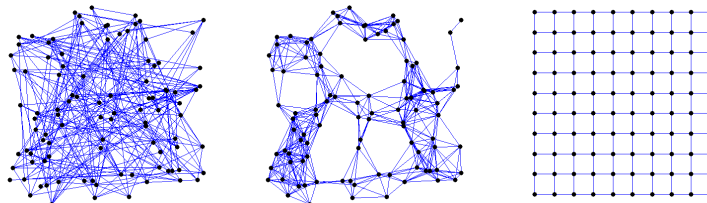


Figure 1: A Erdős-Rényi graph, a Geographic Threshold Graph, and a Lattice Network, each on 100 vertices. In the lattice network, vertices on the top of the graph are adjacent to vertices on the bottom and vertices on the left and right are adjacent.

### 2.1 Erdős-Rényi Graphs

In an Erdős-Rényi graph, the network is formed by creating each possible edge with some constant probability  $p$ . This creates a random graph with approximately  $p|V|$  edges. Though this differs from the method of construction de-

scribed in [5], we can expect the graph to have the same characteristics as the random graphs described therein.

By [3], the diameter of a graph produced this way grows as  $\log(|V|)/\log(p|V|)$ . In particular, a network of size 1000 with  $0.005 \leq p \leq .01$  very probably has a diameter of 3 or 4. This makes these graphs a good example of small world networks, in which, despite individual nodes having relatively few neighbors, there is a low maximum distance between any pair of nodes. Thus while the flow of information is severely restricted in which paths it can take, it does not have to travel through many individuals to permeate the network.

On connected Erdős-Rényi graphs, the same qualitative behavior was observed as in the network-free model. The time to reach equilibrium varied inversely with connectivity but due to the low diameter of the graph did not change drastically. The equilibria states observed were identical to those in the network-free model.

## 2.2 Geographic Threshold Graphs

A Geographic Threshold Graph (GTG) is constructed from a set of  $n$  vertices placed in a space. A nonnegative weight  $w(v)$  is assigned to each vertex. Using a set distance metric  $r(a,b)$ , vertices  $a$  and  $b$  are connected if  $f(w(a),w(b))/r(a,b)^\beta > \theta$  for some fixed threshold value of  $\theta_G$ . One major benefit of this type of network is that it is very easy to visually represent, as vertices tend to be connected to those close to them.

Aside from a few special cases, in the GTG networks we considered, vertices are randomly distributed uniformly on the unit square. Weights are exponential random variables and edges exist between vertices  $a$  and  $b$  if  $(w(a) + w(b))/d(a,b)^2$ . The diameter for such a graph shown in [1] to grow as  $O(\sqrt{n/\log n})$  for graphs that are dense enough to contain a giant component. For the GTGs on 1000 vertices that we used, the average vertex degrees were 3 to 12 and the diameters were between 25 and 55, significantly higher than that of an Erdős-Rényi graph.

A notable difference between Erdős-Rényi graphs and GTGs is that in GTG, clusters of vertices can be densely connected within the cluster yet minimally connected to outside vertices. This allows local phenomena to occur and not quickly spread to the remainder of the network.

On GTGs with a giant component, densely connected subgraphs behave similar to the network-free model, but the network as a whole exhibits distinctly different behavior. Due to the low Cheeger constant for GTGs, metastable equilibria are common.

## 2.3 Lattice Network

The final type of basic network is a four-regular graph built on a torus. In this graph, there are vertices at all lattice points and a vertex is connected to the vertices directly above, below, and on both sides of it. This lattice is placed

on a torus to limit the total size of the network without introducing boundary conditions.

In this lattice network, all vertices are connected in an identical matter and thus no subset of the vertices will experience irregular behavior due to graph topology. The diameter of a lattice network is  $\sqrt{n}$  if the width and height of the torus are equal. Like in GTGs, this method of connection allows for local phenomena that cannot spread to all parts of the graph very quickly. However, unlike GTGs, sets of vertices cannot be relatively isolated and trends cannot “bottleneck” in sparsely connected regions.

## 2.4 Basic Network Comparison

The topological differences between these three networks cause significantly different behaviors. A major factor in this is the concept of distance and isolation.

A graph with a large diameter has a large average distance between two vertices, and thus information takes longer to spread. This spread of information is reflected in the players’ changing strategies. When information spreads slowly, it allows for the formation of localized phenomena. Of all three networks, the Erdős-Rényi random graph is the fastest to converge to a stable equilibrium because of its small diameter; also due to this it does not exhibit localized phenomena.

The main difference between the lattice network and the GTG network is that components of the GTG network can be relatively isolated from the rest of the graph. This allows local phenomena to not only exist but to evolve without spreading to the rest of the network. In the lattice network, no component is isolated, so any local phenomena can expand and eventually encompass the entire network. In a GTG network, this expansion may be prevented by areas of minimal connection. For example, given two complete graphs each on 20 vertices with a single edge between one vertex in the first and one in the second, if the two are at different stable equilibria, it is very difficult for one of these components to convert the other.

## 3 Networks with Weighted Edges

A generalization of the criminal society simulation applies weighted edges to the network. In these networks, an edge weight corresponds to a rate of attack between a pair of players, so some pairs of players are likely to attack each other more often than others. A network with weighted edges allows local phenomena to tend to occur in a specific area without preventing it from slowly spreading to neighboring areas.

### 3.1 Weighted Circular Network

One elementary weighted network we considered was built off a circular structure. Players are arranged in a circular structure and connected with edges

whose weight decreases exponentially as distance around the circle increases. For example, a vertex is connected to the vertices on either side of it with weight  $e^{-\omega}$ , the vertices on the opposite side of those with weight  $e^{-2\omega}$ , etc. In this case, the edge weight describes the rate of attack between a pair of players. In the most basic circular model, these edge weights do not affect the selection of witnesses following a crime.

With this structure, the same types of behaviors as observed in the network-free model are present. The parameter  $\omega$  serves to limit the rate of propagation of information and thus causes time scaling of the rate at which equilibrium will be reached. The case where  $\omega = 0$  is identical to that of a network-free model and behaves accordingly. Additionally, as  $\omega$  grows towards infinity, the propagation of information decreases and causes the rate of change to be so slow as to depend primarily on which player is selected to attack.

The cause of this is that when police-cooperant players are not at a majority and players are significantly more likely to attack the players adjacent to them on a circle, player strategies must propagate linearly. Additionally, when an attacker is not likely to be convicted, Informants attacking Villains are equally likely to convert them to Informants as Villains attacking Informants are to change the Informants to Villains. The primary factor that makes Informants so influential in determining the dynamics of the network-free system is that their attacking Villains creates police-cooperant players. However, if in this network  $\omega$  is too large, if an Informant converts both of his neighbors to Informants, he can no longer convert any more Villains to Informants. This sharply decreases the number of “active” Informants and in fact sets a maximum number of active Informants, because it is extremely unlikely that a chain of Informants will be broken into multiple chains and acquire more ends.

Furthermore, the number of active Villains are limited in the same way. Thus the total number of players active in determining the dynamics of the system is greatly reduced. The number of these active players, however, is persistent because upon the conversion of a vertex on one end of any of these chains, there will be another vertex of the same type behind it, so unless a chain of length 1 is attacked, the number of determining connections does not change. This effect decreases as the number of police-cooperant players increases, as the likelihood of an attacker being convicted increases.

The presence of this slowing effect introduces a new behavior not observed in the network-free model for moderately large values of  $\omega$ . If at any point there is one chain of police-cooperant players (Paladins and Informants) and one opposing chain of police-avoidant players (Villains and Apathetics), the former chain is likely to expand so long as there are Informants on the ends or it contains at least half the circle. Due to the edge weight decay, any small section of the circle can act locally similar to the network-free model, and sections of Informant-Paladin mixes tend to become purely Paladins. In some cases, this causes the entire chain of police-cooperant players to become Paladins before it contains a majority of the players. When this occurs, the simulation is likely to end in dystopia, because a Villain attacking a Paladin has greater than equal odds of not being convicted and thus the Paladin is more likely to become a

Villain. As Paladins do not commit crimes, there is little opposing the Villains consuming the Paladin chain from both ends.

A continuum model for this network can be easily developed due to the highly symmetrical nature of the network. In this case, the edge weight decays exponentially with angle, weight =  $e^{(-\omega\theta)}$ . A set of four partial differential equations was developed to describe the dynamics of this system.

The probability of an attacker being convicted is

$$C(t) = \frac{\int_{-\pi}^{\pi} (P(\alpha, t) + I(\alpha, t)) d\alpha}{2\pi} \quad (1)$$

Additionally, for simplicity we define

$$K(\omega) = \frac{\pi\omega}{1 - e^{-\pi\omega}} \quad (2)$$

Then, the set of equations governing the continuum circle model is

$$\begin{aligned} \frac{\partial}{\partial t} P(\phi, t) = & (I(\phi, t) + V(\phi, t)) K(\omega) \frac{1}{2\pi} \int_{\phi-\pi}^{\phi+\pi} (P(\alpha, t) + I(\alpha, t)) e^{-\omega|\alpha-\phi|} d\alpha \cdot C(t) \cdot \frac{1}{2-\theta} \\ & + I(\phi, t) K(\omega) \frac{1}{2\pi} \int_{\phi-\pi}^{\phi+\pi} (V(\alpha, t) + I(\alpha, t)) e^{-\omega|\alpha-\phi|} d\alpha \cdot (1 - C(t)) \cdot \frac{1-\delta-\epsilon}{2-\epsilon} \\ & - P(\phi, t) K(\omega) \frac{1}{2\pi} \int_{\phi-\pi}^{\phi+\pi} (V(\alpha, t) + I(\alpha, t)) e^{-\omega|\alpha-\phi|} d\alpha \cdot (1 - C(t)) \cdot \frac{1+\delta}{2-\epsilon} \end{aligned} \quad (3)$$

$$\frac{\partial}{\partial t} A(\phi, t) = \left( V(\phi, t) \frac{1-\delta}{2} - A(\phi, t) \frac{1+\delta}{2} \right) K(\omega) \frac{1}{2\pi} \int_{\phi-\pi}^{\phi+\pi} (I(\alpha, t) + V(\alpha, t)) e^{-\omega|\alpha-\phi|} d\alpha \quad (4)$$

$$\begin{aligned} \frac{\partial}{\partial t} I(\phi, t) = & (A(\phi, t) + V(\phi, t)) K(\omega) \frac{1}{2\pi} \int_{\phi-\pi}^{\phi+\pi} I(\alpha, t) e^{-\omega|\phi-\alpha|} d\alpha \frac{1+\delta}{2} \\ & + P(\phi, t) K(\omega) \frac{1}{2\pi} \int_{\phi-\pi}^{\phi+\pi} I(\alpha, t) e^{-\omega|\phi-\alpha|} d\alpha \cdot (1 - C(t)) \cdot \frac{1+\delta}{2-\epsilon} \\ & - I(\phi, t) K(\omega) \frac{1}{2\pi} \int_{\phi-\pi}^{\phi+\pi} (I(\alpha, t) + P(\alpha, t)) e^{-\omega|\phi-\alpha|} d\alpha \cdot C(t) \cdot \frac{1}{2-\theta} \\ & - I(\phi, t) K(\omega) \frac{1}{2\pi} \int_{\phi-\pi}^{\phi+\pi} I(\alpha, t) e^{-\omega|\phi-\alpha|} d\alpha \cdot (1 - C(t)) \cdot \frac{1-\delta-\epsilon}{2-\epsilon} \\ & - I(\phi, t) K(\omega) \frac{1}{2\pi} \int_{\phi-\pi}^{\phi+\pi} V(\alpha, t) e^{-\omega|\phi-\alpha|} d\alpha \cdot C(t) \end{aligned} \quad (5)$$

$$\begin{aligned}
\frac{\partial}{\partial t} V(\phi, t) &= (P(\phi, t) + I(\phi, t)) K(\omega) \frac{1}{2\pi} \int_{\phi-\pi}^{\phi+\pi} V(\alpha, t) e^{-\omega|\phi-\alpha|} d\alpha \cdot (1 - C(t)) \cdot \frac{1 + \delta}{2 - \epsilon} \\
&+ A(\phi, t) K(\omega) \frac{1}{2\pi} \int_{\phi-\pi}^{\phi+\pi} V(\alpha, t) e^{-\omega|\phi-\alpha|} d\alpha \frac{1 + \delta}{2} \\
&- V(\phi, t) K(\omega) \frac{1}{2\pi} \int_{\phi-\pi}^{\phi+\pi} V(\alpha, t) e^{-\omega|\phi-\alpha|} d\alpha \frac{1 - \delta}{2} \\
&- V(\phi, t) K(\omega) \frac{1}{2\pi} \int_{\phi-\pi}^{\phi+\pi} (I(\alpha, t) + P(\alpha, t)) e^{-\omega|\phi-\alpha|} d\alpha \cdot C(t) \cdot \frac{1}{2 - \theta} \\
&- V(\phi, t) K(\omega) \frac{1}{2\pi} \cdot \int_{\phi-\pi}^{\phi+\pi} I(\alpha, t) e^{-\omega|\phi-\alpha|} d\alpha \quad (6)
\end{aligned}$$

$P, A, I$  and  $V$  represent the fraction of the total population of that type at  $\phi$  at time  $t$ . These equations satisfy the following equation, showing that population is conserved.

$$\frac{1}{2\pi} \int_{-\pi}^{\pi} A(\phi, t) + I(\phi, t) + P(\phi, t) + V(\phi, t) d\phi = 1 \quad (7)$$

This continuum model is observed to behave qualitatively similarly to that of the network free model. As the value of  $\omega$  is increased, the system evolves more slowly, though reaches similar final steady states. This reduction in speed of conversion reflects that a high edge rate decay indicates a low rate of transfer of information around the circle, as information is carried by attacks. See Fig. 2.

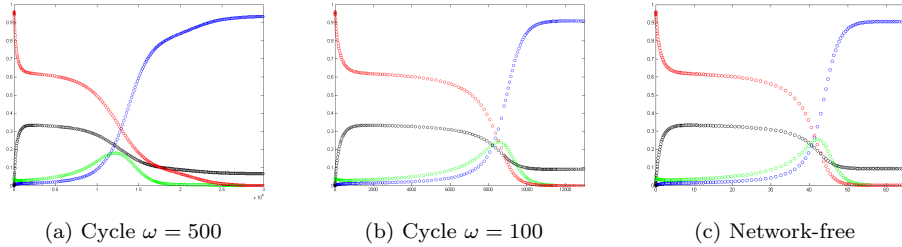


Figure 2: Fig. 2a and 2a show example solutions to Eqns. (3) - (6) with  $\omega = 500$  and  $\omega = 00$  respectively. Initial conditions are: 0.96 Villains and 0.04 Informants, initially placed separated by strategy (ie, the first  $0.04 \cdot 2\pi$  of the circle is Informants and the remainder is entirely Villains). Compare this to a solution for the network-free model in 2c which has similar over all attack rates but a significantly different time scale. Villains are shown in red, Informants in green, Paladins in blue, and Apathetics in black.

## 3.2 Effects of Initial Player Locations

Based on the special properties of the circular network model, we observe how the initial population and its arrangement influence which equilibrium stage is more likely to be reached. From this, we can learn about the potential long-term behavior of a population with different initial distributions of people.

As mentioned before, the larger the value of  $\omega$  is, the more localized any given behavior is. Moreover, when there are more police-avoidant people in the population, the system is more likely to go to dystopia. We investigated the tendency of the society to achieve utopia dependant upon the initial configuration of Informants and the value of  $\omega$ .

We ran the simulation 100 times on a population of size 100, with various initial permutations of Informants and Villains, and with various values of  $\omega$ . We then recorded the number of trials resulting in each of the 2 possible equilibrium states. For example, for an initial population consisting of 4 Informants and 96 Villains (4I+96V), 3 different permutations are constructed: the first permutation had all 4 Informants adjacent to each other and all 96 Villains adjacent to each other; the second had 2 groups of 2 Informants spaced equally between 2 groups of 48 Villains; the third had 4 Informants randomly distributed among the Villains. Similar permutations are constructed for a population containing 6, 10, 15, or 20 Informants.

### 3.2.1 Results

For all values of  $\omega$  for which the utopia equilibrium was achieved, our simulations suggest that the random permutation of Informants and Villains is more likely to result in utopia than the more clustered permutations. There are two properties of the random permutation that likely cause this phenomenon: the average length of the chains of Informants is smaller, and the average edge weight between Villains and Informants is greater. As the number of Informants increases in the initial population, the probability of achieving utopia increases. Moreover, the difference between such probabilities for the random permutation and the clustered permutation become more significant for the cases when initial population contains 10 Informants. For example, when  $\omega = 0.5$ , the sample probabilities of achieving utopia for these permutations with initial population 4I+96V are 20% and 21%, and with initial population 10I+90V, 55% and 39%, respectively.

This result again suggests the influential role that Informants play in affecting the long-term behavior of the population and its probability of reaching utopia [6]. Because of the structure of the circular network, the number of ‘active’ Informants helps determine which equilibrium stage is eventually reached. When  $\omega$  is fixed, the number of neighbors that are more likely to be attacked by each Informant or Villain is fixed as well. When all the Informants are clustered together, only the ones around the two edges of the chain can actively attack police-avoidant players from the opposite chain and possibly increase the number of police-cooperate players in the system. However, when the number

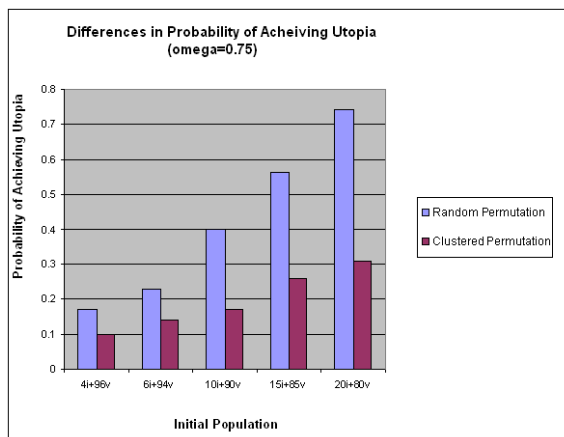


Figure 3: The probabilities of utopia for random and clustered permutation of different initial population,  $\omega = 0.75$ . The probabilities of achieving utopia are generally higher under a random permutation as compared to a clustered permutation.

of Informants is relatively small, this clustered effect may be less significant, because even the Informants in the middle of the chain may still be able to actively interact with the players outside of the chain, and thereby increase the number of police-cooperative players. Therefore, the difference in number of ‘active’ Informants between the clustered permutation and random permutation is not significant, which results in the smaller difference between the probabilities of reaching utopia.

We found that the value of  $\omega$  plays a critical role in determining the likelihood of the system reaching utopia. Given a population of size 100, as  $\omega$  increases from 0.25 to 1.25, the probabilities of achieving utopia decrease regardless of the initial distribution and arrangement of the population. For example, for the initial population 6I+94V arranged randomly, the sample probability of achieving utopia is 39.5% when  $\omega = 0.25$ , compared to 23% when  $\omega = 0.75$ , and 3% when  $\omega = 1.25$ . It also takes longer for the society to reach either equilibrium stage as  $\omega$  increases. When  $\omega \leq 0.75$ , all observed simulations reached an equilibrium state within 300 time steps. However, when  $\omega = 1.5$ , even after 900 time steps, some simulations still failed to reach an equilibrium state. When  $\omega$  is greater or equal to 2, the system takes a significantly greater amount of time to converge.

As  $\omega$  grows, the players become more ‘localized’, which causes the behavior of the population to change much more slowly. This also decreases how ‘active’ the Informants are; there are fewer neighbors that one Informant can attack. The Informants who are inside the chain in the clustered permutation are more likely to change other Informants near them into Paladins, rather than changing players outside of the chain. As mentioned earlier in this section, when the initial

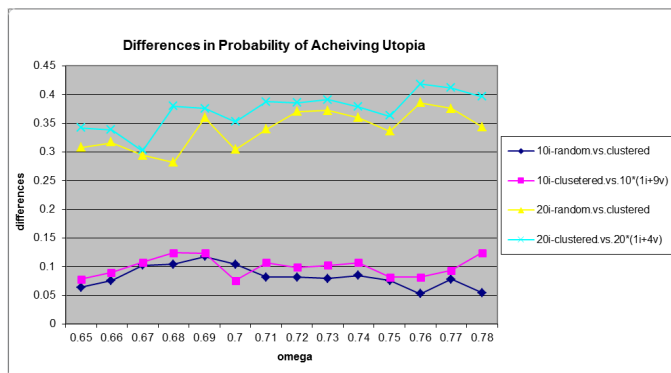


Figure 4: Differences in probabilities of achieving utopia. The notation  $10*(1i+9v)$  and  $20*(1i+4v)$  indicates the equally spaced permutation with average length of Informants equal to 1. The differences in likelihood of achieving utopia are calculated by subtracting the probabilities for a clustered permutation from either a random permutation or the equally spaced permutation.

population is primarily police-avoidant, and the group of police-cooperating players become Paladins before growing to over half of the population, the system is more likely to go to dystopia.

Another interesting behavior we find is that as  $\omega$  increases from 0.25 to around 0.75, the difference between the probabilities of achieving utopia for the random and clustered permutation increases, and the difference decreases as  $\omega$  goes beyond 0.75. We take a closer look at this phenomenon by running the simulation 500 times for initial populations with 10 and 20 Informants under the random and clustered permutations with  $\omega$  incrementing by 0.01 from 0.65 to 0.78. To get a better understanding of what is happening, we also consider the permutation where Informants are equally spaced among the Villains. This again shows that the difference between the probabilities of achieving utopia for the random permutation and clustered permutation is higher in populations with more Informants (figure 4). Moreover, the results for the equally spaced and clustered permutations show a similar pattern. This may not be a coincidence, but we are not able to determine the cause at this time. Further studies and more simulations may be able to give more insight into this behavior. One can also look into the differences in achieving utopia between random permutation and equally spaced permutation in populations consisting of different numbers of Informants.

## 4 An Alternate Interpretation for Edge Weights: Friendliness

Up until this point, edge weights have indicated rates of attack between players. Thus players who are close are likely to attack each other and players who are not likely to attack each other are disconnected. However, edges can instead indicate a friendly connection between two players. Thus two players with a high edge weight are unlikely to attack one another and two distant players - players with a low edge weight - are likely to attack each other.

We can also use this new interpretation to select witnesses for a trial. We assume that a person is more likely to be near people that they are friendly with and thus any potential witnesses of the crime are likely to be connected either to the attacker or the victim. As such, under this edge weight interpretation victims are chosen across low edge weights from the attacker and witnesses are chosen from those having high edge weights with the attacker or victim.

Under this interpretation for edge weights, players who commit crimes benefit from being surrounded by police-avoidant and Paladins benefit from being surrounded by police-compliant players (Apathetics do not benefit from any neighbor makeup because they are never directly involved in any trials). This is because when those neighbors are involved in trials, these witness makeups increase the likelihood that the player is successful in getting acquitted or getting his attacker convicted, respectively.

The functions used to determine attack and witnessing rates from edge weights are monotonic and non-negative to reflect the above properties. Additionally, in order to allow for players to be more distant (lower rate of interaction) these functions are concave up. This allows a minimal rate of interaction, both friendly and unfriendly, at some minimum sum of the two functions. (If, for example, both functions were linear, they would either sum to a constant interaction rate or one type of interaction would correspond to a higher rate of interaction than the other.)

### 4.1 Friendly Edge Weights Applied to the Circle

When this friendly interpretation of edges is applied to the circle network, the dynamics of the system change significantly. The tendency to attack across the circle leads to a pattern appearing in which the makeup of one portion of the circle is reflected by the other side of the circle. As in the previous circle network, the rate of decay of edge weights significantly affects how similar this network is to a network-free model.

For even relatively low values of  $\omega$ , the system quickly becomes relatively stable. This is most easily observed in an example in which we place a set of Informants in consecutive positions while the remainder of the circle is filled with Villains. The game progresses through the following states:

1. Beginning - Informants and Villains are in initial positions.

2. First reflection - Informants attack Villains opposite them, causing them to become Informants (some of the initial Informants become Villains as well).
3. Second reflection - the new Informants attack the original Informants, getting convicted with high probability (because both victim and attacker have majority police-compliant neighbors) and are converted to Paladins; additionally, the original Informants act similarly and are converted to Paladins as well.
4. Unification - any remaining Villains within the pools of Paladins attack Paladins opposite them and are convicted with high probability, leaving the circle divided into four parts: two equal-sized parts of Paladins and two equal-sized parts comprised of a mix of Villains and Apathetics (these four parts need not all be of equal size).

Following this fourth state the system is very stable. That is because any deviation from this state requires a Villain to attack a Paladin. Because Villains and Paladins are not opposite each other, this interaction is most likely to occur on a pair of opposite boundaries. In this case, the neighbors of the attacker will be approximately evenly divided between police-compliant Paladins and police-avoidant Villains and Apathetics; the makeup is similar around the victim. Then, the probability of the attacker being convicted is approximately  $1/2$  and, because the loser is unlikely to mimic his own strategy, whether he is a Paladin or Villain, this reflects the likelihood of conversion.

Now the boundaries of this system approximately follow an unbiased random walk (whether the Paladins or the Villains and Apathetics make up the majority is irrelevant because the majority of all of them will be contained in the interior of a large chain of similar players and thus will not influence the behavior of the boundaries). Thus the system is likely to remain in this state for a very long time. This will terminate once the random walk reduces one of the two classes of players to a critically small mass. At this critical mass, the range of players over which a player on the boundary is likely to draw witnesses contains a second boundary.

## 5 Dynamic Edges

Given that under the friendliness interpretation of edge weights players can benefit from having stronger connections with players with certain strategies, we can allow players to respond to this by determining their edge weights. They can change their edge weights in response to other players' activities. The responses vary by player type and interaction.

Following an attack between two players, their edge weight should decrease, indicating that they are less friendly and future attacks are more likely. Additionally, if they are brought to trial, edge weights with potential witnesses can be affected: the victim will increase their edge weights with players who cooperated with police in the trial and decrease their edge weights with players who

refused to cooperate. Similarly, the attacker will decrease their edge weights with players who cooperated with police and increase their edge weights with players who refused to cooperate with police. These edge weight changes are independent of the outcome of the trial.

There are two possible implementations for dynamic edges, both of which will be discussed here.

## 5.1 Discrete Weights

In the discrete weight implementation, the values for the weights of the edges are initially drawn from a fixed set of possible weights. Then, following an event, edge weights are adjusted by consistent intervals in response to the event, keeping the edge weights in the set of possible weights. For example, a graph may be initialized with edge weights randomly chosen from multiples of 0.2 and, in response to an attack, the following changes occur:

- Edge weight between attacker and victim reduced by 1
- If the case is brought to trial with 5 witnesses
  - Edge weights between attacker and police-compliant witnesses are decreased by 0.4; edge weights between attacker and police-avoidant witnesses are increased by 0.6
  - Edge weights between victim and police-compliant witnesses are increased by 0.6; edge weights between victim and police-avoidant witnesses are decreased by 0.4

The lack of symmetry for positive and negative witness response serves to discourage the overall attack rate for the system from increasing. This would occur because if an attack occurs and is unreported, the only outcome is an increase in attack rate.

To prevent attack rates (and witness rates) from growing without bounds, we impose a lower and upper bound on these edge weights. These bounds are taken at  $\pm 16$ . For a starting edge weight distribution taken uniformly from  $\pm 8$  at intervals of 0.2, these bounds are rarely reached before either utopia or dystopia is reached.

Attack and witness rates are calculated from these edge weights. For a pair of players with edge weight  $w$ , the attack rate is  $e^{-\alpha w}$  and the witness rate is  $e^{\beta w}$ . This allows there to be a minimum rate of interaction where the edge weight is zero - here a pair of players are neither likely to attack each other nor be called on as witnesses in each other's trials.

One of the most easily observed deciding factors in determining the behavior of these systems is the amount by which an edge weight is changed following a negative interaction. If these changes are minimal, the system will behave qualitatively like the network-free system. If these changes are large, the system quickly reaches a metastable state in which pairs or small sets of players form strongly negative edge weights and, as a result, only attack a very small number

of people (in many cases only one person). In this case, any developments in such a set of negatively connected players are largely contained in that set of players and will not spread to the remainder of the graph. It remains to be seen if these metastable states eventually evolve to predictable final states.

In cases where the above mentioned edge changes are between these small and large values, more simulations are necessary to predict trends in behavior.

## 5.2 Continuous Weights

An alternate approach to dynamic edges allows players to have variable responses to crimes. While in this case negative responses are uniformly negative and positive responses are uniformly positive, the magnitude of change can depend on the current edge weight. This reflects how a person may be more likely to have a stronger reaction to the actions of a person they are close to than one they are more distant from. For example, if Person A's close friend refuses to cooperate as a witness in a trial for a crime against Person A, Person A would likely respond more negatively than if the pair were very distant and did not know each other.

This approach to dynamic edges takes the interaction strength into account when determining the magnitude of the reaction. Insufficient data has been gathered to determine the effects of such an edge-changing strategy.

## 6 Stationary Distributions

In order to verify the solution of the ordinary differential equations presented by Short et. al. [6] we considered a society where only Villains and Apathetics remain. The number of Villains  $X_n$  in this population of total size  $T$  can be considered as a Markov birth and death chain. We can construct the transition matrix as follows:

$$p(k, k+1) = \begin{cases} \left(\frac{T-k}{T-1}\right)\left(\frac{1+\delta}{2}\right) & 1 \leq k < T \\ 0 & k = 0 \end{cases}$$

$$p(k, k-1) = \left(\frac{k-1}{T-1}\right)\left(\frac{1-\delta}{2}\right) \quad 1 \leq k \leq T$$

$$p(k, k) = \begin{cases} \left(\frac{k-1}{T-1}\right)\left(\frac{1+\delta}{2}\right) + \left(\frac{T-k}{T-1}\right)\left(\frac{1-\delta}{2}\right) & 1 \leq k \leq T \\ 1 & k = 0 \end{cases}$$

These entries are placed in a transition matrix

$$\mathbf{P} = \begin{pmatrix} p(0,0) & p(0,1) & 0 & 0 & 0 & \dots & 0 \\ p(1,0) & p(1,1) & p(1,2) & 0 & 0 & \dots & 0 \\ 0 & p(2,1) & p(2,2) & p(2,3) & 0 & \dots & 0 \\ \vdots & \vdots & \vdots & \vdots & \vdots & \ddots & \vdots \\ 0 & 0 & 0 & 0 & \dots & p(T, T-1) & p(T, T) \end{pmatrix}$$

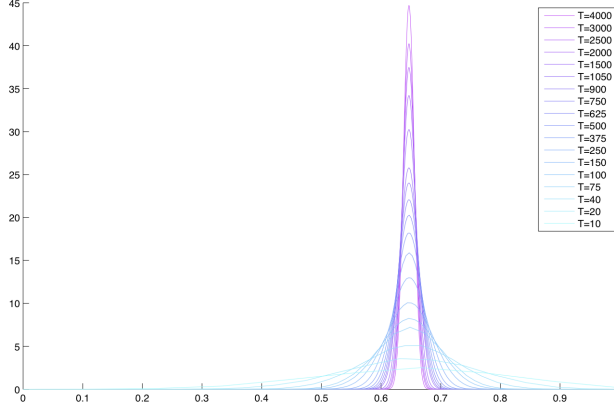


Figure 5: Set of stationary distributions of proportion of Villains in society. For these,  $\delta = 0.3$ .

We can then find the stationary distribution for this system by solving the system of equations

$$\begin{aligned} \vec{\pi} \mathbf{P} &= \vec{\pi} \\ \sum_{i=0}^T \pi(i) &= 1 \end{aligned}$$

which can be rewritten as

$$\begin{aligned} (\mathbf{P}' - I)\pi' &= 0 \\ \sum_{i=0}^T \pi(i) &= 1 \end{aligned}$$

This system of  $T + 1$  equations in  $T$  variables is then fed into a Jacobi Iterative solver with initial guess  $\vec{0}$ , and a tolerance of  $10^{-4}$  under the  $l_{\text{inf}}$  norm. The solution  $\vec{\pi}$  was found, and the points  $(\frac{i}{T}, \pi(i) \cdot (T))$  were plotted. The additional factor of  $T$  was added in order to renormalize the distribution so that the Riemann sum of the distribution is 1, allowing us to visualize the different distributions as the total population changes. We note that as the population increases, the stationary distribution approaches the Dirac delta function centered at  $\frac{1+\delta}{2}$ .

## 7 Distribution of Wealth

### 7.1 Alterations to the Model

In order to create a concept of wealth in this society the following changes were made to the simulation:

- Each individual is given a certain wealth that they maintain from attack to attack. If an individual gains or loses any value from their wealth, that is carried over to later attacks.
- Each attack steals a portion  $\delta$  of the wealth of another person. For example, if person A has wealth 0.8, person B has wealth 2, and  $\delta = 0.3$ , then if person A attacks person B and succeeds, person A will take 0.6 wealth from person B, and the new wealths will be 1.4 for person A and person B.
- When a person is convicted they lose a certain portion of their wealth as opposed to a fixed value. For example, if person A has wealth 0.8 and  $\epsilon = 0.2$ , then person A is convicted, person A will lose 0.16 from their wealth, and be at 0.64 for future attacks.
- Similarly, when a person is not convicted, but is brought to trial, the victim loses a portion of their wealth as opposed to a fixed value. For example, if person B's wealth after an attack is 1.4 and  $\theta = 0.2$ , person B will lose 0.28 from their wealth, bringing their final wealth to 1.12 for future attacks.
- The loser of an attack is now defined as the person whose difference  $Wealth_{final} - Wealth_{initial}$  is less. This will universally lead to the victim of a non-reported attack, the victim in an attack where the attacker is not convicted, and the attacker when the attacker is convicted.
- The loser of the encounter will chose their new strategy based upon the total wealth held by each person. For example if person A (Villain) attacks person B (Apathetic), with the final wealths being 2.4 and 0.6 respectively, then person B is the loser (victim of a non-reported attack) and will emulate person A (become a Villain) with probability  $\frac{2.4}{3.0} = 0.8$ , while they will remain Apathetic with probability  $\frac{0.6}{3.0} = 0.2$ .
- At the end of each attack, every person in the society increases their wealth by some interest term. For example, if person C has wealth 1.0 before a given attack, it had been 0.5 time units between attacks, and the "interest rate" is 0.5%, then after this attack person C's wealth will be 1.0025.

These differences allow for a more realistic model of society, where individuals can accumulate wealth and will likely continue to do what has made them financially successful. If a Villain has accumulated a lot of wealth, they are likely to remain a Villain even when they lose an encounter as their net worth will be much higher than their attacker.

## 7.2 Results of Simulations on Erdős-Rényi Graphs

### 7.2.1 Probability of connection of 1

A total of 1,730 simulations on fully connected (any two nodes connected with probability 1), uniform probability of attack networks were run under these

new rules starting with 40 Informants, 0 Paladins, 960 Villains, and 0 Apathetics (to be notated  $[40, 0, 960, 0]$ ), where the initial wealth of each person is 1. Of these simulations, 1,230 went to utopia, while 500 went to dystopia. We then constructed a confidence interval, and thus we are 98% confident that the true proportion of societies initialized with  $[40, 0, 960, 0]$  is between 0.2643 and 0.3150.

We also computed the Gini Coefficient [4] utilizing a trapezoidal approximation for the integral of the Lorentz curve for each society. The mean Gini Coefficient for utopias was found to be 0.4488 with a standard deviation of 0.01, while the mean Gini Coefficient for dystopias was found to be 0.3817 with a standard deviation of 0.0086. We then performed a one tailed, two-sample t-test on these samples with a 98% confidence level. We used:

$$\begin{aligned} H_0 &: \mu_{utopia} - \mu_{dystopia} = 0 \\ H_A &: \mu_{utopia} - \mu_{dystopia} > 0 \end{aligned}$$

We used a pooled degrees of freedom of 1,068.9, found the t-score to be 140.8857, and produced a p-value of  $p \approx 0$ . Because  $p < 0.02$ , we are able to reject the null hypothesis and conclude that  $\mu_{utopia} - \mu_{dystopia} > 0$ .

This t-test strongly suggests that the Lorentz curves for utopias lie below the Lorentz curves of dystopias, indicating that wealth is more evenly distributed in a dystopia than in a utopia. In order to confirm this we performed a set of 2-sample t-tests on each lattice point of the Lorentz curves. For each of these, assuming 1000 people in the population, for  $k = 1, 2, \dots, 998, 999$ , we used the null hypothesis

$$\begin{aligned} H_0 &: \text{The least wealthy } \frac{k}{10}\% \text{ of the population in a utopia controls the same} \\ &\quad \text{proportion of the society's wealth as the least wealthy } \frac{k}{10}\% \text{ of a dystopia} \\ H_A &: \text{The least wealthy } \frac{k}{10}\% \text{ of the population in a utopia controls a lower} \\ &\quad \text{proportion of the society's wealth as the least wealthy } \frac{k}{10}\% \text{ of a dystopia} \end{aligned}$$

At each of these 999 lattice points, the p-value was found to be less than  $p = 10^{-88}$ , which is significantly less than 0.02. We are able to reject each of the null hypotheses and conclude for each  $k$  that the least wealthy  $\frac{k}{10}\%$  of the population in a utopia controls a lower proportion of the society's wealth as the least wealthy  $\frac{k}{10}\%$  of a dystopia.

This statistical analysis also strongly suggests that wealth is more evenly distributed in dystopia than in utopia.

### 7.2.2 Probability of connection of 0.5

We also ran a total of 974 simulations on an Erdős-Rényi graph with the probability of each pair of nodes being connected is 0.5, with uniform probability of attack, under initial conditions  $[38, 0, 706, 0]$  and initial wealth 0 for each person. Of these simulations 724 went to utopia, while 250 went to dystopia.

The Gini Coefficient was also calculated for each of these simulations, and the mean Gini Coefficient for utopias was found to be 0.4489 with a standard

deviation of 0.0115, while the Gini Coefficient for dystopias was found to be 0.3806 with a standard deviation of 0.0089. We then performed a one tailed, two-sample t-test on these samples with a 98% confidence level. We used:

$$\begin{aligned} H_0 &: \mu_{utopia} - \mu_{dystopia} = 0 \\ H_A &: \mu_{utopia} - \mu_{dystopia} > 0 \end{aligned}$$

We used a pooled degrees of freedom of 555.3050, found the t-score to be 96.6386, and produced a p-value of  $p \approx 0$ . Because  $p < 0.02$ , we are able to reject the null hypothesis and conclude that  $\mu_{utopia} - \mu_{dystopia} > 0$ .

### 7.2.3 Probability of connection of 0.1

We also ran a total of 1,055 simulations on an Erdős-Rényi graph with the probability of each pair of nodes being connected is 0.1, with uniform probability of attack, under initial conditions [38, 0, 706, 0] and initial wealth 0 for each person. Of these simulations 805 went to utopia, while 250 went to dystopia.

The Gini Coefficient was also calculated for each of these simulations, and the mean Gini Coefficient for utopias was found to be 0.4498 with a standard deviation of 0.0120, while the Gini Coefficient for dystopias was found to be 0.3806 with a standard deviation of 0.0095. We then performed a one tailed, two-sample t-test on these samples with a 98% confidence level. We used:

$$\begin{aligned} H_0 &: \mu_{utopia} - \mu_{dystopia} = 0 \\ H_A &: \mu_{utopia} - \mu_{dystopia} > 0 \end{aligned}$$

We used a pooled degrees of freedom of 517.5506, found the t-score to be 94.1796, and produced a p-value of  $p \approx 0$ . Because  $p < 0.02$ , we are able to reject the null hypothesis and conclude that  $\mu_{utopia} - \mu_{dystopia} > 0$ .

### 7.2.4 Probability of connection of 0.05

We also ran a total of 1,069 simulations on an Erdős-Rényi graph with the probability of each pair of nodes being connected is 0.05, with uniform probability of attack, under initial conditions [38, 0, 706, 0] and initial wealth 0 for each person. Of these simulations 819 went to utopia, while 250 went to dystopia.

The Gini Coefficient was also calculated for each of these simulations, and the mean Gini Coefficient for utopias was found to be 0.4510 with a standard deviation of 0.0116, while the Gini Coefficient for dystopias was found to be 0.3812 with a standard deviation of 0.0116. We then performed a one tailed, two-sample t-test on these samples with a 98% confidence level. We used:

$$\begin{aligned} H_0 &: \mu_{utopia} - \mu_{dystopia} = 0 \\ H_A &: \mu_{utopia} - \mu_{dystopia} > 0 \end{aligned}$$

We used a pooled degrees of freedom of 412.516, found the t-score to be 83.276, and produced a p-value of  $p \approx 0$ . Because  $p < 0.02$ , we are able to reject the null hypothesis and conclude that  $\mu_{utopia} - \mu_{dystopia} > 0$ .

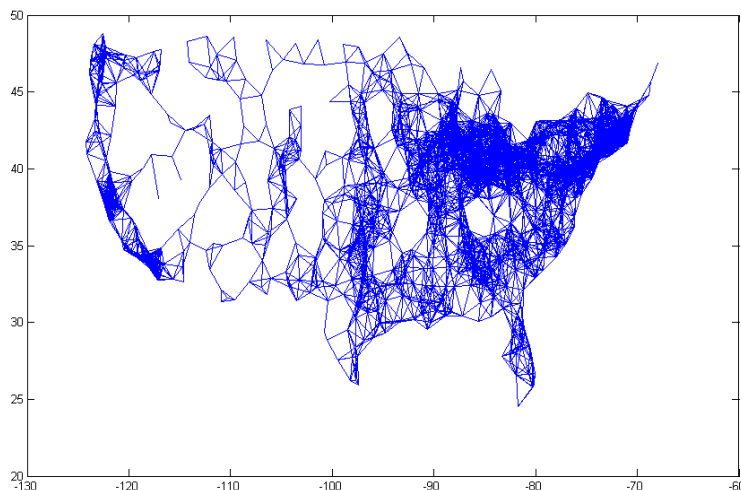


Figure 6: Geographic Threshold map of the USA used for the various simulations

### 7.3 Creation of a GTG Network

In order to create an interesting GTG network, we took the positions (latitude and longitude) of 744 major cities across the contiguous United States. We applied a geographic thresholding algorithm to this set of points where cities located nearby to each other were connected with higher probability. Once this was completed we ensured that the graph was connected by manually adding 1 edge between the singular disconnected point and another local point on the map. This mapping procedure created a variety of interesting topologies in differing regions of the map:

- In the Northeast near Boston, New York City and Philadelphia, we find that these cities are nearly fully connected, and so these regions will act as if they are a fully connected system.
- In California, there are major areas around Los Angeles and San Francisco that are themselves nearly fully connected and connected to each other by a few nodes.
- In the Idaho and Montana area, there are a number of cities that are connected to each other by a few connections, and connected to the rest of the country by only two or three nodes.
- In the North Dakota area there are a series of cities that are connected in a pattern that appears to be like a triangular lattice, leading to a back and forth of non-witnessing and witnessing in the area.

## 7.4 Results of Simulations on Geographic Threshold Graph

We ran a total of 168 simulations with initial conditions  $[38, 0, 706, 0]$  where individuals kept the wealth gained from each attack, of which 103 resulted in utopia, while 65 resulted in dystopia. The mean Gini coefficient in utopia was found to be 0.6259 with a standard deviation of 0.0569, while the mean Gini coefficient in dystopia was found to be 0.4302 with a standard deviation of 0.1151. We will use  $\mu_u$  and  $\mu_d$  to represent the true mean of the Gini coefficient of utopia and dystopia respectively. A two sample t-test with confidence level 0.98 was performed with:

$$\begin{aligned}H_0 &: \mu_u - \mu_d = 0 \\H_A &: \mu_u - \mu_d > 0\end{aligned}$$

The two sample t-test produced a t-value of 12.7525, which was then calculated against a t-distribution with 84.0131 degrees of freedom to find a p-value of approximately 0. We are thus able to reject the null hypothesis and conclude that the mean Gini coefficient in utopia is higher than the mean Gini coefficient in dystopia.

## 7.5 Results of Simulation on a 4-Regular Network

We ran a total of 92 simulations with initial conditions  $[42, 0, 742, 0]$  where individuals kept the wealth gained from each attack, of which 34 resulted in utopia, while 58 resulted in dystopia. The mean Gini coefficient in utopia was found to be 0.6799 with a standard deviation of 0.0612, while the mean Gini coefficient in dystopia was found to be 0.4450 with a standard deviation of 0.1107. We will use  $\mu_u$  and  $\mu_d$  to represent the true mean of the Gini coefficient of utopia and dystopia respectively. A two sample t-test with confidence level 0.98 was performed with:

$$\begin{aligned}H_0 &: \mu_u - \mu_d = 0 \\H_A &: \mu_u - \mu_d > 0\end{aligned}$$

The two sample t-test produced a t-value of 13.102, which was then calculated against a t-distribution with 89.778 degrees of freedom to find a p-value of approximately  $1.5 * 10^{-22}$ . We are thus able to reject the null hypothesis and conclude that the mean Gini coefficient in utopia is higher than the mean Gini coefficient in dystopia.

## 7.6 Differences Between the Network-Free Model and GTG Networks

We ran a total of 325 simulations with initial conditions  $[38, 0, 706, 0]$  on network-free model where individuals kept the wealth gained from each attack. 236 of these resulted in utopia, while 89 of these resulted in dystopia. The mean Gini coefficient in utopia was found to be 0.4480 with a standard deviation of 0.0121,

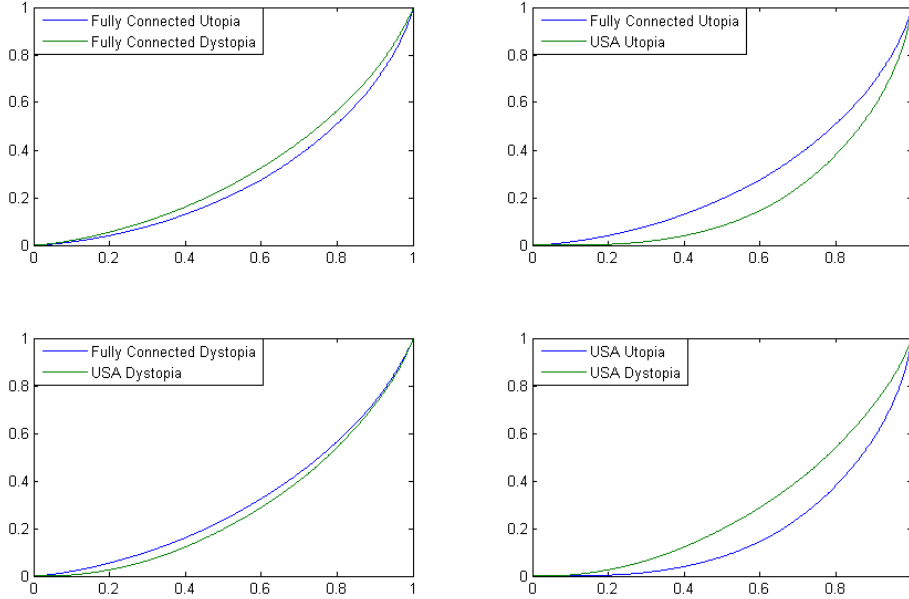


Figure 7: Set of sample Lorenz curves generated from these simulations. Each curve was selected so that its Gini coefficient was very near the typical Gini coefficient for those parameters. The curves labeled “USA Utopia” and “USA Dystopia” represent societies which evolve on the GTG network of the United States, while “Fully Connected Utopia” and “Fully Connected Dystopia” represent societies which evolve on fully connected networks.

while the mean Gini coefficient in dystopia was found to be 0.3809, with a standard deviation of 0.0095.

We will use  $p_f$  and  $p_g$  to represent to the true proportion of societies in utopia in network-free and GTG network model respectively. In order to determine if this GTG network model tends towards utopia at a different rate than the fully connected graphs we ran a two proportion p-test with confidence level 0.98 was performed with:

$$\begin{aligned}
 H_0 &: p_f = p_g \\
 H_A &: p_f \neq p_g
 \end{aligned}$$

The test was performed with  $\widehat{p}_f = \frac{236}{325}$ ,  $n_f = 325$ ,  $\widehat{p}_g = \frac{103}{168}$ , and  $n_g = 168$ . This test produced a z-score of 2.5672, which translates to a p-value of 0.0051. We are thus able to reject the null hypothesis and conclude that the proportion of network-free societies that go to utopia is less than that of the proportion of societies on GTG networks.

We also performed two-sample t-tests to determine if the Gini coefficient for utopias in a network-free model is different than the Gini coefficient for utopias in the GTG network model, and to determine if the Gini coefficient for dystopias

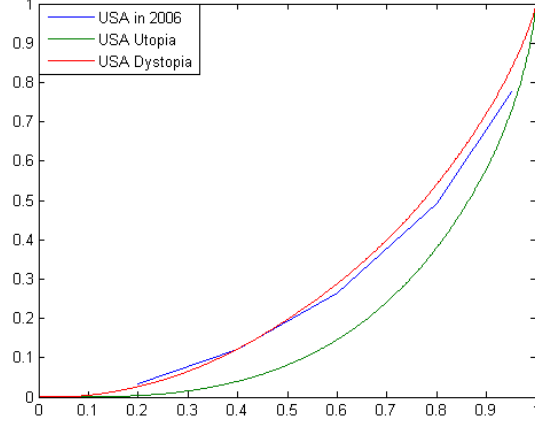


Figure 8: A comparison between the actual Lorenz distribution of the United States and sample generated utopian and dystopian distribution[2].

in a network-free model is different than the Gini coefficient for dystopias in a GTG network model. The two-sample t-tests were performed with a confidence level of 0.98 with:

$$\begin{aligned}
 H_0 &: \mu_{u_f} - \mu_{u_g} = 0 \\
 H_A &: \mu_{u_f} - \mu_{u_g} < 0
 \end{aligned}$$

and

$$\begin{aligned}
 H_0 &: \mu_{d_f} - \mu_{d_g} = 0 \\
 H_A &: \mu_{d_f} - \mu_{d_g} < 0
 \end{aligned}$$

The first t-test produced a t-value of 31.4223, which was then calculated against a t-distribution with 106.0481 degrees of freedom to find a p-value of  $7.5970 * 10^{-56}$ . We are thus able to reject the null hypothesis and conclude that the mean Gini coefficient in utopia in a network-free model is less than the mean Gini coefficient in utopia in the GTG network model.

The second t-test produced a t-value of 3.3748, which was then calculated against a t-distribution with 64.6373 degrees of freedom to find a p-value of  $6.2652 * 10^{-4}$ . We are thus able to reject the null hypothesis and conclude that the mean Gini coefficient in dystopia in a network-free model is less than the mean Gini coefficient in dystopia in the GTG network model. Our findings for the Gini Coefficient in various scenarios are summarized in figure 9.

	Utopia			Dystopia		
	Mean	S. D.	Count	Mean	S. D.	Count
Fully Connected	0.4480	0.0121	236	0.3809	0.0095	89
0.5 Connectivity	0.4489	0.0115	724	0.3806	0.0089	250
0.1 Connectivity	0.4498	0.0120	805	0.3806	0.0095	250
0.05 Connectivity	0.4510	0.0116	819	0.3812	0.0116	250
0.01 Connectivity	0.4749	0.0134	86	0.3752	0.0091	53
Geographic Threshold	0.6259	0.0569	103	0.4302	0.1151	65
4-regular	0.6799	0.0612	34	0.4450	0.1107	58

Figure 9: This table shows the Gini Coefficient for each of the sets of simulations except the 4-regular system run on  $[38, 0, 706, 0]$  systems. The 4-regular system was run on initial conditions  $[42, 0, 742, 0]$

## 8 Results and Discussions

Overall it was determined that many network adaptations of the model introduced by Short et al. behave qualitatively similarly to the network-free model. The connectivity of these networks is highly influential in the time scales over which these models evolve. In particular, a large graph diameter corresponds to a large time scale.

On networks that have structures conducive to localized behavior, metastable states may be observed with stability inversely related to connectivity. Models on such networks can exhibit behaviors distinct from those in the network-free model, such as the collapse of a police-compliant chain on the circular network. The existence of the potential for these behaviors may lead to distinct proportions of stable states reached by simulations on different networks. Specifically, the potential for highly localized behavior may reduce the likelihood for a simulation to terminate in utopia.

We are able to conclude in each of the previously mentioned scenarios (Geographically Threshold, fully connected, Erdős-Rényi and 4-regular graphs) that the wealth is more evenly distributed when the society reaches dystopia. This can be attributed to the increased number of attacks to achieve dystopia causing the wealth to be more evenly spread out, as individuals are more likely to have their wealth taken, and less likely to report it stolen, giving them a chance to recover it. Our data also loosely suggests that as the diameter of the graph increases, as coordinated with a decrease in the connection probability in Erdős-Rényi graphs, the Gini Coefficient in both utopia and dystopia will increase as well. This may be due to individuals protecting their wealth by forming a buffer of non-attackers around them, and so persons with low wealth are unlikely to attack persons with higher wealth. Further studies are necessary to confirm this phenomenon, where additional probabilities of connection are to be tested, and the graph is ensured to be connected. It may also be useful to compare the distributions of wealth produced along various other diameter controlled networks.

## References

- [1] Milan Bradonjić, Aric Hagberg, and Allon G. Percus. The structure of geographical threshold graphs. In *9 M. Bradonjic' and Joseph Kong, Wireless Ad Hoc Networks with Tunable Topology, Proceedings of the 45th Annual Allerton Conference on Communication, Control and Computing*, 2007.
- [2] B. D. Proctor C. DeNavas-Walt and J. Smith. *Income, Poverty, and Health Insurance Coverage in the United States: 2006*. US Census Bureau, 2007.
- [3] F. Chung and L. Lu. The diameter of sparse random graphs. *Adv. in Appl. Math.*, 26:257–279, 2001.
- [4] R. Dorfman. A formula for the gini coefficient. *The Review of Economics and Statistics*, 61(1), 1979.
- [5] P. Erdős and A. Rényi. On the evolution of random graphs. *Magyar Tud. Akad. Mat. Kutató Int. Közl.*, 5, 1960.
- [6] P.J. Brantingham M. B. Short and M.R. D Orsongna. Cooperation and punishment in an adversarial game: How defectors pave the way to a peaceful society. *Physical Review E*, 82(6), 2010.
- [7] J. Von Neumann. *Theory of Games and Economic Behaviors*. Princeton University Press, 1944.
- [8] G. Tsebelis. Penalty has no impact on crime: A game-theoretic analysis. *Rationality and Society*, 2(3), 1990.